

Dalton Transactions

Accepted Manuscript



This article can be cited before page numbers have been issued, to do this please use: A. Raya-Baron, C. P. Galdeano-Ruano, P. Oña-Burgos, A. Rodríguez Diéguez, R. Langer, R. López-Ruiz, R. Romero-González, I. Kuzu and I. Fernández, *Dalton Trans.*, 2018, DOI: 10.1039/C8DT01123K.



This is an Accepted Manuscript, which has been through the Royal Society of Chemistry peer review process and has been accepted for publication.

Accepted Manuscripts are published online shortly after acceptance, before technical editing, formatting and proof reading. Using this free service, authors can make their results available to the community, in citable form, before we publish the edited article. We will replace this Accepted Manuscript with the edited and formatted Advance Article as soon as it is available.

You can find more information about Accepted Manuscripts in the [author guidelines](#).

Please note that technical editing may introduce minor changes to the text and/or graphics, which may alter content. The journal's standard [Terms & Conditions](#) and the ethical guidelines, outlined in our [author and reviewer resource centre](#), still apply. In no event shall the Royal Society of Chemistry be held responsible for any errors or omissions in this Accepted Manuscript or any consequences arising from the use of any information it contains.



Journal Name

ARTICLE

A New Anthraquinoid Ligand for the Iron-catalyzed Hydrosilylation of Carbonyl Compounds at Room Temperature: New Insights and Kinetics

Received 00th January 20xx,
Accepted 00th January 20xx

DOI: 10.1039/x0xx00000x

www.rsc.org/

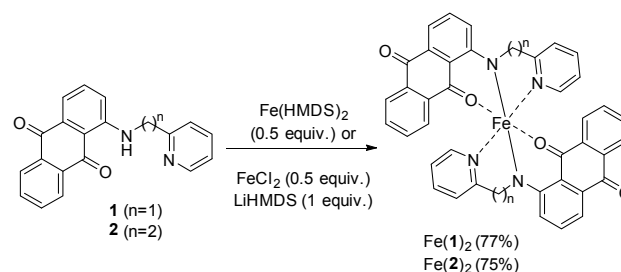
Álvaro Raya-Barón,^a Carmen P. Galdeano-Ruano,^a Pascual Oña-Burgos,^a Antonio Rodríguez-Diéguez,^b Robert Langer,^c Rosalía López-Ruiz,^a Roberto Romero-González,^a Istemi Kuzu^c and Ignacio Fernández^{*c}

The reaction of 1-((2-(pyridin-2-yl)ethyl)amino)anthraquinone with either $\text{Fe}(\text{HMDS})_2$ or $\text{Li}(\text{HMDS})/\text{FeCl}_2$ allowed the preparation of a new anthraquinoid-based iron(II) complex active in hydrosilylations of carbonyls. The new complex $\text{Fe}(\mathbf{2})_2$ was characterized by single-crystal X-ray diffraction, infrared spectroscopy, NMR and high resolution mass spectrometry (electrospray ionization). Superconducting quantum interference device (SQUID) magnetometry established no spin crossover behavior with an $S = 2$ state at room temperature. This complex was determined to be an effective catalyst for the hydrosilylation of aldehydes and ketones, exhibiting turnover frequencies of up to 63 min^{-1} with a broad functional group tolerance by just using 0.25 mol % of catalyst at room temperature, and even under solvent-free conditions. The aldehyde hydrosilylation renders it one of the most efficient first-row transition metal catalyst for this transformation. Kinetic studies have proven first-order dependences with respect to acetophenone and Ph_2SiH_2 and a fractional order in the case of the catalyst.

Introduction

The reduction of carbonyl groups into alcohols is a widely used transformation in organic chemistry, employed in the industry as well as in the academic field.¹ This type of transformation is frequently used as an early stage evaluation towards the development of catalytic systems for the reduction of CO_2 .² Among the different methodologies currently available, hydrosilylation has proved to be a convenient method to convert a carbonyl function into an alcohol via a silyl ether intermediate,³ which can also be useful as protecting group in synthesis.⁴ Since the seminal works by Piers on Frustrated Lewis Pairs,⁵ non-transition-metal-catalyzed hydrosilylations have been developed.⁶ However, this reaction has been traditionally carried out using second- and third-row transition metals as catalysts.^{3,7} The high cost or toxicity of these metals have motivated the research for new catalysts based on earth-abundant non-toxic first-row transition metals.⁸ In this respect, iron meets the requisites of being inexpensive,

environmentally benign and less toxic than its relatives.⁹ Consequently, many iron-based catalytic systems for the hydrosilylation of carbonyl compounds have been reported in recent years,^{10,19,23} but only few of them work at room temperature and use low catalyst loadings ($\leq 1 \text{ mol } \%$). For instance, iron(0) NHC carbene complexes of $\text{Fe}_3(\text{CO})_{12}$, provide excellent conversions of hydrosilylated aldehydes at room temperature with 1 mol % within a few hours.¹¹ A more impressive system is the one developed by Tilley and coworkers,¹² which employed an iron silylamide complex in concentrations as low as 0.01 % to achieve similar results. In both cases, the source of hydrogen is always primary or secondary silanes. Chirik and coworkers investigated defined iron dialkyl complexes of pybox ligands and bisoxazoline at 0.3 mol % of concentration in the hydrosilylation of carbonyl compounds with excellent yields.¹³



Scheme 1. Synthesis of anthraquinone-based iron complexes $\text{Fe}(\mathbf{1})_2$ and $\text{Fe}(\mathbf{2})_2$.

^a Department of Chemistry and Physics, Research Centre CIAIMBITAL, Universidad de Almería, Ctra. Sacramento s/n, 04120 Almería, Spain.

^b Department of Inorganic Chemistry, Faculty of Science, University of Granada, 18070 Granada, Spain.

^c Department of Inorganic Chemistry, Fachbereich Chemie, Philipps-Universität Marburg, Hans-Meerwein-Straße 4, 35032 Marburg, Germany.

Electronic Supplementary Information (ESI) available: [Experimental procedures, spectral and crystallographic data (PDF). Crystallographic data for **2** (CIF). Crystallographic data for $\text{Fe}(\mathbf{2})_2 \cdot 0.5\text{thf}$ (CIF)]. See DOI: 10.1039/x0xx00000x

ARTICLE

Journal Name

Due to its advantageous electronic structure and reversible redox activity, the anthraquinone unit has found numerous applications when incorporated in transition metal complexes.¹⁴ Interestingly, the catalytic activity of these complexes is scarce, and even more pronounced when the iron metal is involved. We have already developed an anthraquinone-based iron(II) catalyst $\text{Fe}(\mathbf{1})_2$ (Scheme 1) for the hydrosilylation of acetophenone as a preliminary work in this field.¹⁵ Very good conversions were obtained at room temperature in short times, although the transformation of acetophenone into 1-phenylethanol didn't reach complete conversion. To overcome the catalytic performance of this previous iron complex, we describe herein a more flexible ligand that significantly improves the catalytic properties of its iron complex, which represents one of the most active catalysts in hydrosilylations of carbonyls described so far.

Results and Discussion

In the quest of alternative anthraquinone-based ligands, we envisaged the synthesis of a more flexible chelate which would assist the catalytic process by allowing the easy access of the substrates to the iron center. We then synthesized *N*-(ethylene-2-pyridine)-1-aminoanthraquinone (ligand **2**, Scheme 1) from 1-chloroanthraquinone and 2-(2-aminoethyl)pyridine via a simple and quick reaction in good yields. Importantly, the method allows the recovery of most of the unreacted 1-chloroanthraquinone for its reuse. The procedure followed is a modification of the one described by Barasch *et al.*,¹⁶ where we were able to reduce the amount of solvent and employ a minor excess of aminoethylpyridine. All the details regarding its NMR characterization (including two-dimensional ^1H , ^{13}C and ^{15}N NMR) together with its X-ray crystallographic data can be found in the supporting information. The ^1H NMR spectrum of the ligand shows a diagnostic signal attributed to the NH resonance at δ_{H} 9.89 ppm, due to hydrogen-bonding with the C=O moiety. Among many other ^{13}C NMR features, we highlight the hydrogen-bonded and non-bonded carbonyls with signals at δ_{C} 185.0 and 183.9 ppm, respectively. The FT-IR bands located at 3272 and 1626 cm^{-1} corroborates further this intra-molecular hydrogen bonding (Figure S13). ^1H , ^{15}N gHMBC experiments optimized for $1/J_{\text{NH}}$ of 83.3 ms (Figure 1), allowed the assignment of two nitrogens at δ_{N} 84.4 (NH) and 308.6 ppm for the aminoanthraquinone and pyridine units, respectively.

In the solid state, the X-ray crystal structure of **2**, grown by hexane diffusion in a dichloromethane solution, confirms the chelating potential of the ligand given the intramolecular hydrogen bond between NH and C=O (quinone) of 1.888(2) Å (Figure S20). This interaction produced a carbonyl bond slightly longer (C9-O1, 1.235(2) Å) than the one found for the non-hydrogen-bonded case (C10-O2 1.222(2) Å). In the solid state, the torsion angle between the pyridine plane and the aminic moiety (N1-C17-C16-C15) of 178.9(13)° shows an inadequate chelate conformation. As in the case of ligand **1**, anthraquinone moieties of **2** are oriented in the crystal network in a face-to-face disposition with an inter-planar

distance of ca. 3.45 Å (centroid-centroid distance), establishing π -stacking arrangements (Figures S19).^{15,17}

The reaction of ligand **2** and $\text{Fe}(\text{HMDS})_2$ allowed us to obtain complex $\text{Fe}(\mathbf{2})_2$ in crystalline pure form in 75% isolated yield. Interestingly, the iron silylamide reagent deprotonates the aminic ligand and introduces the metal centre in a single step (Scheme 1). Alternatively, complex $\text{Fe}(\mathbf{2})_2$ can be synthesized by using LiHMDS as a base and FeCl_2 as the iron(II) source. This method resulted also effective but with a slightly lower isolated yield of 64 %.

Despite its paramagnetism, the ^1H NMR spectrum of complex $\text{Fe}(\mathbf{2})_2$ in $\text{THF-}d_8$ was partially assigned. It exhibits 11 resonances attributable to a C_2 symmetric compound with signals in the range of δ_{H} -43.6 to 57.3 ppm. The most up-field signal appears as a rather broad resonance almost indiscernible from the noise with a half line width ($W_{1/2}$) of 1955 Hz.

When the same reaction is performed with 1.0 equiv. of $\text{Fe}(\text{HMDS})_2$ instead of half of it, a new set of signals is observed. This new species shows 13 resonances consistent with a C_1 paramagnetic complex tentatively assigned to a 1:1 stoichiometry species such as $\text{Fe}(\mathbf{2})\text{HMDS}$. The resonances with highest and lowest frequencies were located at δ_{H} 128.3 and -79.1 ppm, respectively. Interestingly, there is a signal of prominent intensity at δ_{H} 12.6 ppm ($W_{1/2}$ = 457 Hz) that was assigned to the 18 protons associated with the $\text{N}(\text{HMDS})_2$ moiety consistent with the assignment. Figure 1 shows the ^1H NMR spectra for both complexes. Unfortunately, all the attempts to isolate the 1:1 complex failed, always obtaining only complex $\text{Fe}(\mathbf{2})_2$ instead.

These evidence prompted us to study the one to one stoichiometry reaction in more detail. ^1H NMR monitoring of this reaction at ambient temperature showed that the group of signals attributed to complex $\text{Fe}(\mathbf{2})_2$ increased with increasing reaction time, which also produced the progressive diminution of the relative concentration of complex $\text{Fe}(\mathbf{2})\text{HMDS}$.

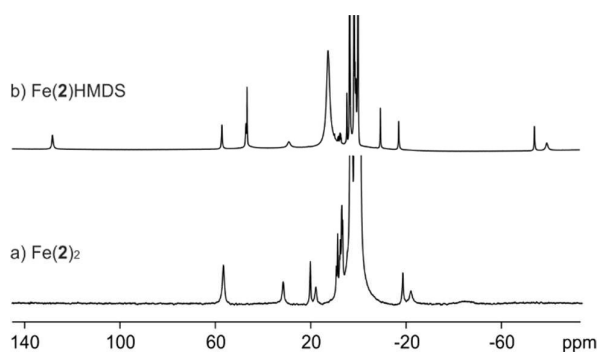


Figure 1. ^1H NMR (500 MHz) spectra of complexes $\text{Fe}(\mathbf{2})_2$ and $\text{Fe}(\mathbf{2})\text{HMDS}$ in $\text{THF-}d_8$ at room temperature.

From a 1:8 ratio between $\text{Fe}(\mathbf{2})_2$ and $\text{Fe}(\mathbf{2})\text{HMDS}$, respectively, at the beginning of the reaction, we ended up with a 1:2 ratio after 4 days at room temperature, that kept constant over the following days. At this point, we decided to heat the sample up to 60 °C and monitor both species within time. To our surprise,

after 16 hours no modification of the equilibrium ratio was observed what is consistent with a high activation energy between these two species. Anyhow, all these findings support the existence of a thermodynamic equilibrium between both complexes, with the former being the most stable species for the stoichiometry employed. Single crystals of complex $\text{Fe}(\mathbf{2})_2$ were also grown and analyzed by X-ray diffraction. The complex crystallizes with a solvent molecule as $\text{Fe}(\mathbf{2})_2 \cdot 0.5\text{thf}$. A view of the complex is shown in Figure 2. Selected crystal data and bond lengths and angles are given in Table S3.

In the complex, the ethylenic unit is rearranged adopting a pseudo-*gauche* conformation with a torsion angle N1-C15-C16-C17 of $76.4(6)^\circ$. Another major change observed in the conformation of $\mathbf{2}$ upon coordination of iron(II) is the loss of planarity of the anthraquinone; the three-rings system completely planar in the free ligand, is now bent around an axis defined by the two carbonyl groups. The lack of coplanarity together with the elongation of 0.030\AA of the metal-coordinated C=O bond (Table S3), is ascribed to an increased sp^3 hybridization character of C9. The reduced angle of $115.7(5)^\circ$ for O1-C9-C12 in the complex compared to the ligand together with the slight reduction on the N1-C1 distance bond, support the latter statement. These two features are highly consistent with a partial delocalization of the negative charge from the amide to the aromatic ring.

The geometry around the metal center can be described as a distorted octahedron that can be viewed as a *mer* isomer, i.e. the two tridentate ligands contain both *trans* (O1/N2 and O3/N4) and *cis* (O1/N1 and O3/N3) pairs (Figure 2). A total of four six-membered metalla rings are defined in the structure, two of them established in the chelation of each ligand.

The metalla rings that involves the anthraquinone moiety resembles a quite planar conformation where only the Fe atom is out of the plane by 0.89 and 0.90\AA , respectively. The other metalla ring, built through the more flexible ethylenic bridge displayed a twist-boat conformation. Interestingly, significant differences are found between $\text{Fe}(\mathbf{2})_2$ and our previously described pre-catalyst $\text{Fe}(\mathbf{1})_2$,¹⁵ when their solid-state structures are carefully inspected.

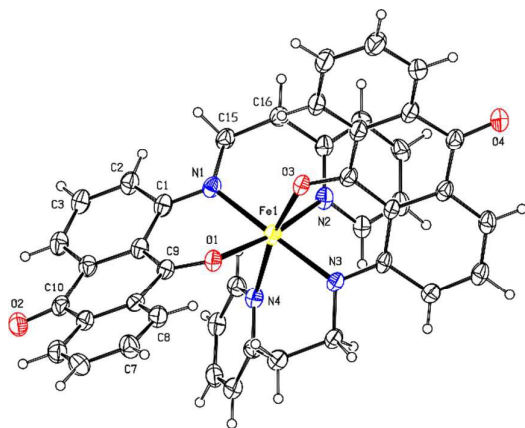


Figure 2. X-ray diffraction structure of complex $\text{Fe}(\mathbf{2})_2$. ORTEP view with ellipsoids at 30% probability level. Co-crystallizing solvent molecule omitted for clarity.

Complex $\text{Fe}(\mathbf{1})_2$ displays two six-membered and another two five-membered metalla rings, all of them with highly planar conformation,¹⁵ and thus with a more rigid backbone than that one found in $\text{Fe}(\mathbf{2})_2$, which would make it more difficult to accommodate any incoming substrate. From this perspective complex $\text{Fe}(\mathbf{2})_2$ is expected to behave as a more reactive pre-catalyst than its former analogue.

The FT-IR spectra (Figure S14) in THF solution showed two C=O stretching bands at 1643 and 1579 cm^{-1} , indicating the unsymmetrical coordination of the two quinone oxygens in solution.

The cyclic voltammogram of $\text{Fe}(\mathbf{2})_2$ in THF exhibits two quasi-reversible reduction waves at -1.54 and -2.08 V versus Fc/Fc⁺ couple (Fc = ferrocene), which were assigned to the reduction of the anthraquinone moiety of the coordinated ligand (Figure 3). In comparison to the uncoordinated $\mathbf{2}$ the reduction waves are shifted to more negative potentials, providing further evidence for the coordination of the anthraquinone group in solution. An irreversible oxidation wave with a peak potential of 0.80 V and a quasi-reversible oxidation wave at 0.91 V are attributed to the oxidation of iron(II) and one of nitrogen-containing donor groups.

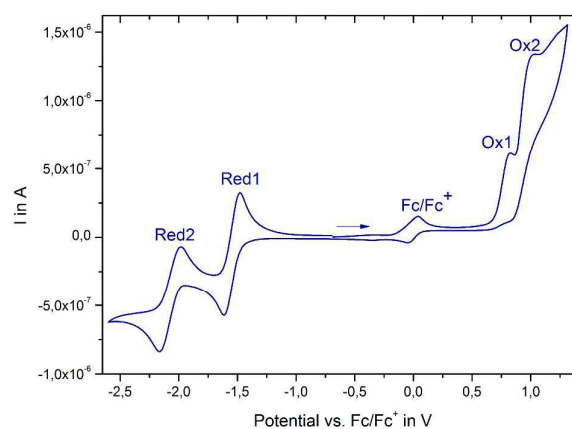


Figure 3. Cyclic voltammogram of complex $\text{Fe}(\mathbf{2})_2$ in THF (1 mM, scan rate 100 mV/s , Pt/ $0.2\text{ M } n\text{-Bu}_4\text{NPF}_6$ /Pt).

Apart from its crystallographic and potentiometric characterization, MS spectrometry was used to verify the structural nature of $\text{Fe}(\mathbf{2})_2$ in more detail. The positive ESI mode revealed a parent ion corresponding to $[\text{C}_{42}\text{H}_{30}\text{FeN}_4\text{O}_4]^+$ with m/z of 710.16465 , that fits the solid state structure. As expected, the observed isotopic cluster pattern matches well with the calculated one (Figures S15 and S16).

The magnetic properties of $\text{Fe}(\mathbf{2})_2$ were studied by variable temperature solid-state SQUID magnetometry in the temperature range of $2\text{--}300\text{ K}$ (Figure S21). Data were collected on three independently prepared, analytically pure samples, and the individual runs were indistinguishable. The variable-temperature magnetic properties indicate that there is no spin crossover behavior observable in the temperature range from 2 to 300 K . At 300 K , $\chi_{\text{M}}T$ equals $2.91\text{ cm}^3\text{ mol}^{-1}\text{ K}$ which established an average molar magnetic susceptibility (χ_{M}) of $0.0097\text{ cm}^3\text{ mol}^{-1}$, consistent with a doublet ground

ARTICLE

Journal Name

state, 3.92 (~4) unpaired electrons, and therefore a high-spin Fe(II) electronic configuration. When the temperature is lowered, χ_{MT} remains constant down to ~30 K. Below this temperature, χ_{MT} decreases reaching a value of 1.20 cm³ mol⁻¹ K at 2 K, which can be attributed to very weak antiferromagnetic interactions just as other works have reported.¹⁸

Hydrosilylation of carbonyl compounds

We started our study of the catalytic performance of Fe(2)₂ in carbonyl hydrosilylation by screening different hydrosilanes as reducing agents and varying the catalyst loading. The benchmark carbonyl was acetophenone (Table 1). From our previous experience using Fe(1)₂ as pre-catalyst,^[15] we expected the hydrosilylation process to occur at room temperature in THF with a catalyst need below 1 mol %. We first tested the most inexpensive silanes such as Et₃SiH and PMHS, which showed undetectable (entry 2) or poor (entry 3) hydrosilylation conversions. With Me₂PhSiH as silane, the catalytic activity was also undetectable (entry 4), which shows than even introducing an aryl group in the silane did not affect the outcome under the conditions assayed.

Table 1. Optimization of the reaction conditions for the hydrosilylation of acetophenone.^[a]

Entry	Silane	Cat. (mol %)	Time (h)	Conv. (%)
1	Ph ₂ SiH ₂	0.50	1	56
2	Et ₃ SiH	0.50	1	0
3	PMHS	0.50	1	13
4	Me ₂ PhSiH	0.50	1	0
5	PhSiH ₃	0.50	1	99
6	(EtO) ₂ MeSiH	0.50	1	94 (>99) ^[b]
7	(EtO) ₂ MeSiH	0.50	2	>99 (81) ^[c]
8	(EtO) ₂ MeSiH	0.25	1	86
9	(EtO) ₂ MeSiH	0.25	2	92
10	(EtO) ₂ MeSiH	0.05	1	37
11	(EtO) ₂ MeSiH	0.05	14	91

[a] Reaction conditions: acetophenone (0.56 mmol), silane (0.63 mmol), THF (2 mL), room temperature. Catalyst percentage relative to the carbonyl substrate. Quenched with aqueous 1M HCl (2 mL). Conversions were determined by ¹H-NMR of the reaction crude. Control experiments using only ligand 1 as catalyst were performed without product formation. [b] In parenthesis is shown the conversion of the run without THF. [c] Isolated yield in parenthesis.

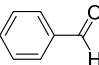
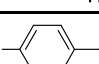
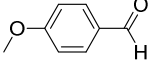
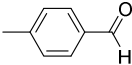
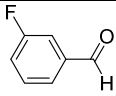
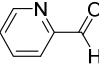
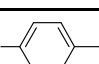
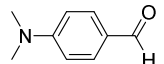
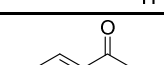
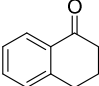
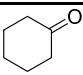
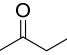
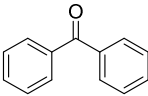
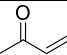
The best results among the selected reductants were achieved with PhSiH₃ and (EtO)₂MeSiH (entries 5 and 6). Remarkably, (EtO)₂MeSiH yielded complete carbonyl reduction (>99% as judged by ¹H NMR spectroscopy) of acetophenone in two hours (entry 7). The TOF value for this transformation at 68% of conversion was 1632 h⁻¹ (27.2 min⁻¹), which is a significant value in the range of the best iron-based catalysts but still far from those provided by Stradiotto and Turculet of 393 min⁻¹,¹⁹ or those reported by Trovitch and coworkers (>14850 h⁻¹) with transition metals others than iron.²⁰

Lowering the loading of catalyst down to 0.25 mol % still allowed excellent conversions of silyl ethers (entries 8-9). The use of 0.05 mol% of catalyst resulted in the need of

considerably longer reaction times, obtaining a 91% of conversion after 14 hours (entry 11, Table 1). The reaction proved to be also valuable under solvent-free conditions (entry 6), even improving the conversion obtained in solution from 94% to >99%. It is also worth mentioning that no additive other than our complex Fe(2)₂ in catalytic amount, was needed for the reactions to take place.

The substrate scope was explored using (EtO)₂MeSiH as the reducing agent of choice, at 0.50 mol % of iron catalyst Fe(2)₂ and at room temperature as the optimized conditions set. The catalytic outcome was excellent for the reduction of aromatic and aliphatic ketones as well as for sterically demanding substrates. The reaction with benzaldehyde (entry 1, Table 2) was so quick at 0.50 mol % Fe(2)₂ load that we were not able to record its ¹H-NMR spectrum before it was fully converted. The TOF values obtained at 95% of conversion was of 38 min⁻¹.

Table 2. Iron-catalyzed hydrosilylation of aldehydes and ketones using Fe(2)₂.^[a]

Entry	Substrate	Cat. (mol %)	Time (min)	Conv. (%) ^[c]
1		0.50	10	>99
2		0.25	30	>99 (90)
3		0.25	5	>99 (89)
4		0.25	5	>99 (90)
5		0.25	20	>99 (88)
6		0.25	5	7
7		0.25	60	>99 (78)
8		0.25	5	79
9		0.25	25	>99 (77)
10		0.50	120	98 (58)
11		0.50	120	94 (79)
12		0.50	120	90 (69)
13		0.50	120	83 (41)
14		0.50	120	31

[a] Reaction conditions: ketone or aldehyde (0.56 mmol), silane (0.63 mmol), THF (2 mL), room temperature. Catalyst percentage relative to the carbonyl substrate. Quenched with aqueous 1M HCl (2 mL). Conversions were determined by ¹H-NMR of the reaction crude. [c] Isolated yield in parenthesis.

To the best of our knowledge these turn-over frequencies represent one of most rapid found for iron-catalyzed

hydrosilylations of carbonyls at room temperature, albeit not always identical experimental conditions are compared. We thus decided to bring the catalyst loading down to 0.25 mol % for the comparative study of the whole set of aldehydes. Under these conditions the conversion obtained was again quantitative but in 30 minutes of reaction time (entry 2, Table 2). For benzaldehyde derivatives, we found that electron-donating substituents located at the *para* position decreased the reaction times down to 5 minutes for complete hydrosilylation (entries 3-4, Table 2), and that with electron-withdrawing substituents such as fluorine, almost no effect was observed (entries 5, Table 2). In the case of nitrogen-based substrates such as picolinaldehyde and 4-dimethylaminobenzaldehyde, extended reaction times were necessary to reach full conversion, with 60 minutes for the former and 25 minutes for the latter (entries 6-9, Table 2). A plausible reason for this reaction retardation is the coordination of these nitrogen-based moieties to the metal center that could compete with substrate coordination. The alkane functionality of ketone substrates such as 3,4-dihydronaphthalen-1(2H)-one (entry 10, Table 2), cyclohexanone (entry 11, Table 2) and 2-butanone (entry 12, Table 2) produced excellent conversions but within 2 hours of reaction times. We should consider that this decreased activity is because, in general, ketones react slower than the corresponding reaction of aldehydes. This could arise from an increased steric component and the less electrophilic carbonyl carbon atom, which was supported by the lower conversion of 83% obtained in the case of benzophenone (entry 13, Table 2) after 2 hours of reaction. Substrates containing both carbonyl group and C-C double bond were also assayed showing a significant decreased on reactivity (entry 14, Table 2). Hydrosilylation of esters, amides, cyano and alkenes were attempted, but no reaction product was observed under similar conditions to those used for ketones and aldehydes. Thus, these functional groups are not expected to interfere with the reduction of aldehydes or ketones if present in the same molecule. Carboxylic acids, alcohols or primary amines are not compatible with the strong basic character of complex $\text{Fe}(\mathbf{2})_2$.

Regarding the nitro function, hydrosilylation of 4-nitrobenzaldehyde was carried out, but very little conversion into the corresponding alcohol was obtained, presumably due to competing interaction of the NO_2 group with the iron center in the catalyst. No product derived from the reduction of the nitro group was detected either.

The reactivity of some of these substrates was monitored by ^1H -NMR spectroscopy in J-Young NMR tubes. These reaction profiles are shown in Figure 4 and allowed us to distinguish the maximum rates and culmination steps. We did not observe the characteristic induction periods in the fastest catalysis but in the case of the slowest, i.e. benzophenone, a characteristic induction period of approximately 25 minutes was observed. The intersection of the maximum rate tangent with the abscissa was taken as the time required for the catalyst activation (Figure 4).²¹ Further experiments focused on

registering a better activation step for other ketones were unsuccessful due to very broad signals in the NMR spectra.

To rule out the formation of iron nanoparticles as the catalytically active species, we performed one of the already reported methods for differentiating between hetero- and homogeneous catalysts. The experiment is called the "fractional poisoning experiment",²¹ and uses less than one equivalent of a poisoning reagent such as trimethylphosphine. In our case, we reproduced entry 7 in Table 1 but using 0.5 equivalents of phosphine relative to our pre-catalyst $\text{Fe}(\mathbf{2})_2$. Interestingly, the reaction was not poisoned completely and proceeded *ca.* two times slower than without phosphine. In fact, the observed rate mimicked the one catalyzed with only 0.25 mol % of catalyst. For comparison issues we provide in Figure S27 the kinetic profile when the loading of catalyst is of 0.50 mol %.

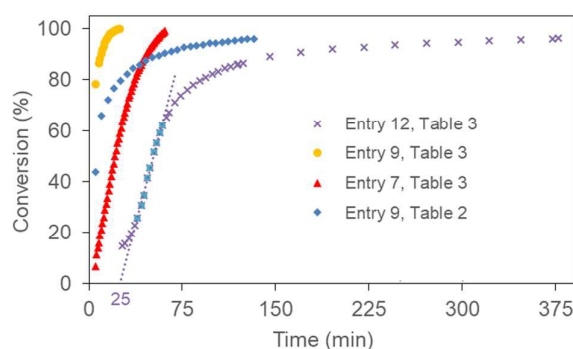


Figure 4. Reaction profiles of the catalytic hydrosilylation of acetophenone, picolinaldehyde, 4-dimethylaminobenzaldehyde and benzophenone, all of them using $(\text{EtO})_2\text{MeSiH}$ as silane and $\text{Fe}(\mathbf{2})_2$ as catalyst.

These observations support the hypothesis that the active catalytic species is our new anthraquinonic homogeneous complex and not any heterogenous system that could have formed during the elapsed time such as surface atoms of nanoparticles. Such nanoparticles have explained prolonged induction periods in many metal-catalyzed processes which are accepted as constituted by two steps, i.e. slow nucleation and then fast agglomeration.^[22]

To examine the repeatability of the transformation, we performed eight consecutive catalytic runs of the hydrosilylation of acetophenone on a J-Young NMR tube (entry 7, Table 1) with only one loading of catalyst (0.5 mol %). No significant loss of catalytic activity was observed after eight reaction cycles, where conversions higher than 99% for all the successive cycles were determined by ^1H NMR. Remarkably, the reaction crude in all the cycles remained clean without forming significant amounts of side products.

Kinetic study

In order to determine the rate law of the reaction, we varied the concentration of each component of the reaction, following a similar methodology than the one described by Bleith and Gade.²³ For the reduction of acetophenone with $(\text{EtO})_2\text{MeSiH}$, we found that the initial rate of the reaction was not appreciably affected as a function of acetophenone

ARTICLE

Journal Name

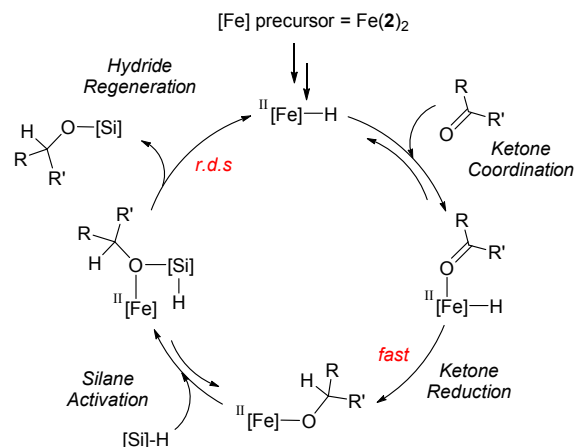
concentration, indicating a zeroth order dependence on ketone concentration (Figure 5a, line in triangles).

However, when the same set of experiments were performed using the non-coordinating Ph_2SiH_2 instead of $(\text{EtO})_2\text{MeSiH}$, the initial rate of the reaction showed a positive linear correlation with the acetophenone concentration, indicating first order dependence in this case (Figure 5a, line in circles).

When we tried to ascertain the reaction order on silane, and varied the concentration of $(\text{EtO})_2\text{MeSiH}$, we found that the initial rate of the reaction decreased as the silane concentration increased (line in triangles, Figure 5b). However, when the same experiments were performed using Ph_2SiH_2 as the reducing agent, we found again a positive linear correlation between the initial rate of the reaction and the silane concentration what again corroborates a first order dependence (Figure 5b). The intersection of the linear fit in the latter was found to be not displaced from the origin which is sign that there was no consumption of silane during precatalyst activation. When we represent the initial rate of 1-phenylethan-1-ol (acetophenone reduction product) versus pre-catalyst concentration in the range of 0.05 to 0.5 mol %, using either $(\text{EtO})_2\text{MeSiH}$ or Ph_2SiH_2 (Figure 5c), we found in both cases positive linear correlations with slopes of ca. 0.4 in the Ln-Ln graphs (Figure S22-S25). At present, the exact reason for this observed fractional rate-orders is not clear and will require further rationalization. From these kinetic data, the rate law for the iron-catalyzed hydrosilylation of ketones is given by the following equation.

$$\frac{d[P]}{dt} = k \cdot [\text{Fe}(2)_2]^{0.4} \cdot [\text{Ph}_2\text{SiH}_2]^1 \cdot [\text{Ketone}]^1$$

The above findings lead us to propose a mechanistic cycle for the iron-catalyzed hydrosilylation as depicted in Scheme 2. It matches previous studies,¹⁵ where four main steps are suggested: (i) coordination of the ketone (in equilibrium), (ii) reduction of the ketone (fast); (iii) silane activation (in equilibrium), and (iv) Fe-hydride regeneration and product release. The first-order dependences with respect to acetophenone and Ph_2SiH_2 implies that the rate-determining-step is the latter, which involves an intermediate that comprises both the ketone and the silane, so when deriving the rate law, first orders result.



Scheme 2. Mechanistic proposal for the Fe(II)-catalyzed hydrosilylation of ketones.

In the diethoxymethylsilane case, there must be a secondary process that participates in the activation step, inactivating further the metal center as the concentration of silane increases, i.e. ethoxy coordination. We actually had observed a similar phenomenon with our previously reported complex $\text{Fe}(1)_2$,¹⁵ when we carried out stoichiometric experiments in the quest of intermediates species derived from the use of catalyst. When 1 equivalent of $(\text{EtO})_2\text{MeSiH}$ is added to a solution of $\text{Fe}(1)_2$ in $\text{THF}-d_8$ and the reaction is monitored by ^1H -NMR, the appearance of a new set of paramagnetic signals is observed along a 24 hours period. When a second equivalent of $(\text{EtO})_2\text{MeSiH}$ is added to the mixture, a progressive increase of a new set of signals together with the complete disappearance of the resonances corresponding to $\text{Fe}(1)_2$ after another 24 hours is noticed (Figure S12).

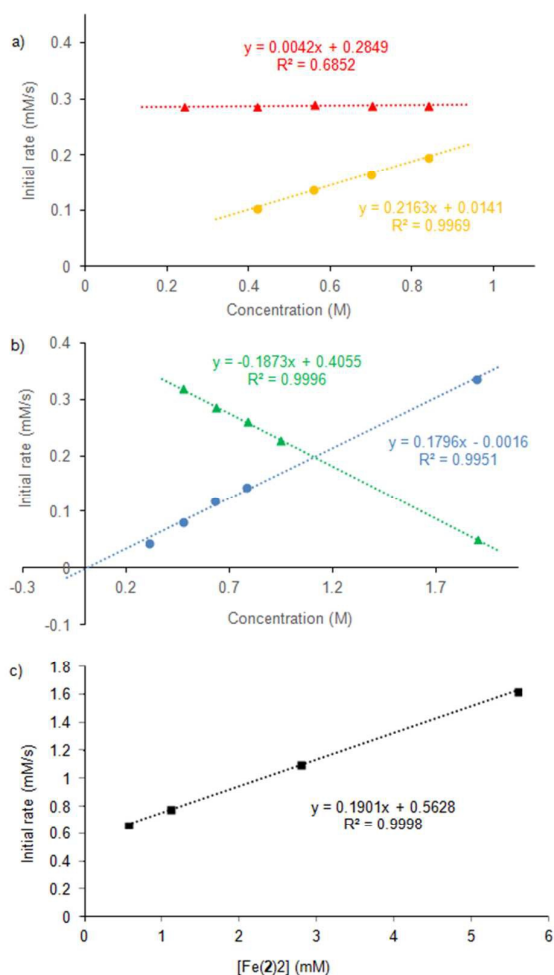


Figure 5. a) Initial rate as a function of concentration of acetophenone using $(\text{EtO})_2\text{MeSiH}$ (red triangles) and Ph_2SiH_2 (orange circles); b) Initial rate as a function of concentration of $(\text{EtO})_2\text{MeSiH}$ (green triangles) and Ph_2SiH_2 (blue circles); c) Initial rate as a function of concentration of pre-catalyst $\text{Fe}(\text{Z})_2$ using Ph_2SiH_2 as reducing agent.

This new complex shows a similar paramagnetic behavior exhibiting 10 signals in the range from δ_{H} -56.1 to 95.0 ppm. High-resolution mass spectrometry (electrospray ionization) experiments confirmed this new species to be consistent with a complex that contains two molecules of $(\text{EtO})_2\text{MeSiH}$ together with the $\text{Fe}(\text{1})_2$ entity. The presence of a molecular ion at m/z 950.28919 corroborates the formation of this new complex. As expected, the observed isotope pattern matches well with the one calculated for the exact mass of $[\text{C}_{50}\text{H}_{54}\text{FeN}_4\text{O}_8\text{Si}_2]$ (Figure S17-18). The accurate molecular structure and how these two silane molecules are attached to the iron center remain unknown since all the attempts to obtain crystals suitable for X-ray analysis were unsuccessful. To determine that the new species arises from silane coordination and not from the hydrosilylation of the quinonic carbonyls in ligand **1**, a sample of this new complex $[\text{Fe}(\text{1})_2\{(\text{EtO})_2\text{MeSiH}\}_2]$ was hydrolyzed with diluted aqueous HCl. After extraction of the organic components with ethyl acetate, ligand **1** was recovered unaltered, from which we concluded that the

$(\text{EtO})_2\text{MeSiH}$ molecules are involved in Fe coordination as no irreversible reaction of the ligand was evidenced. In any case, to prove why the initial rate of the reaction did not linearly increase with the diethoxymethylsilane concentration, we screened the catalytic performance of $[\text{Fe}(\text{1})_2\{(\text{EtO})_2\text{MeSiH}\}_2]$ by adding acetophenone in the reaction media. To our surprise, no hydrosilylation products nor any transformation of the starting materials were appreciated by ^1H NMR under these conditions.

The addition of 10 equivalents of $(\text{EtO})_2\text{MeSiH}$ together with 10 more of acetophenone did not conduct to any transformation either, proving $[\text{Fe}(\text{1})_2\{(\text{EtO})_2\text{MeSiH}\}_2]$ to be completely inactive in hydrosilylation, and therefore corroborating that no rate dependence with this diethoxysilane could be observable.

Interestingly, when these two equivalents are added to complex $\text{Fe}(\text{2})_2$, we were not able to detect any new species and only slow degradation of the complex into a crowded uncharacterized mixture was observed. Even more, when simultaneously to the diethoxymethylsilane were added acetophenone, complete desired product formation was immediately observed, proving the much more reactive the complex is when ligand **2** is chelating the metal center, than when ligand **1** is involved.

Experimental Section

General procedures of laboratory

All air-sensitive experiments were performed under an inert atmosphere of N_2 using standard Schlenk techniques or a glovebox. Deuterated solvents were degassed and dried over activated molecular sieves prior to use. DMSO was dried by distillation from anhydrous CaH_2 and then stored over activated 4 Å molecular sieves. 2-(2-aminoethyl)pyridine was distilled from KOH under reduced pressure before use. 1-Chloroanthraquinone was purchased from Aldrich and used as received. THF and hexane were dried and degassed via elution through a solvent column drying system.²⁴ $\text{Fe}(\text{HMDS})_2$ was synthesized by a method previously described in literature.²⁵ LiHMDS and FeCl_2 were purchased from ABCR and used as received. All hydrosilanes employed in the catalytic runs were purchased from Acros and used without further purification. All ketones and aldehydes used for catalysis were purified and dried by standard methodologies prior to use.²⁶ Triethylamine was distilled from CaH_2 and degassed. NMR spectra were measured in Bruker Avance III 300 and Bruker Avance III 500 spectrometers. IR spectra were recorded in a FT-IR Bruker Alpha spectrometer. Mass spectra were acquired with and Orbitrap mass spectrometer (Thermo Fischer Scientific). Elemental analyses (EA) were performed on a Elementar vario EL cube in the CHN mode. Magnetization and variable temperature (2-300 K) magnetic susceptibility measurements on polycrystalline samples were carried out with a Quantum Design SQUID device operating at different magnetic fields. Values of the magnetic susceptibility were corrected for the underlying diamagnetic increment using tabulated Pascal

constants and the effect of the blank sample holders (gelatin capsule/straw).

Synthesis of ligand **2**

Ligand **2** was synthesized modifying a previously described method.¹⁶ To a pre-heated solution of 1-chloroanthraquinone (2 g, 8.1 mmol) in dry DMSO (20 mL), 2-(2-aminoethyl)pyridine (2 mL, 16.7 mmol) was added and the resulting solution stirred at 150 °C for 10 minutes. The solution was then poured into cold water (200 mL) and the red precipitate was filtered out and washed with water. The pure product was obtained as a red powder after flash chromatography on silica gel using EtOAc/*n*-hexane (1:1) as eluent. Yield: 1.34 g (50%). Suitable crystals for X-ray diffraction were grown by layering a dichloromethane solution of **2** with hexane. M.p. 124.8 °C. ¹H NMR (500.13 MHz, CDCl₃): δ (ppm) 10.89 (1H, bs, NH), 8.63 (1H, d, *J* = 4.2 Hz, H-21), 8.29 (1H, dd, *J* = 1.5 Hz, 7.5 Hz, H-8), 8.25 (1H, dd, *J* = 1.5 Hz, 9 Hz, H-5), 7.78 (1H, ddd, *J* = 1.5 Hz, 7.2 Hz, 7.5 Hz, H-7), 7.72 (1H, ddd, *J* = 1.8 Hz, 7.5 Hz, 7.5 Hz, H-6), 7.67 (1H, dd, *J* = 1.8 Hz, 7.5 Hz, H-19), 7.62 (1H, dd, *J* = 1.5 Hz, 7.5 Hz, H-4), 7.56 (1H, dd, m, H-3), 7.25 (2H, m, H-18, H-20), 3.82 (2H, dt, *J* = 7.1, 5.4 Hz, H-16), 3.25 (2H, t, *J* = 7.1 Hz, H-15). ¹³C-NMR (125.76 MHz, CDCl₃): δ (ppm) 185.0 (CO, C9), 183.9 (CO, C10), 158.8 (C17), 151.3 (C1), 149.7 (C21), 136.3 (C19), 135.3 (C3), 135.0 (C12), 134.7 (C14), 133.9 (C7), 133.0 (C6), 132.9 (C11), 126.7 (C8), 126.7 (C5), 123.6 (C19), 121.8 (C18), 117.9 (C2), 115.8 (C4), 113.1 (C13), 42.8 (C16), 37.8 (C15). ¹⁵N NMR (500.13 MHz, CDCl₃, via gHMBC): δ 84.4, 308.6 ppm. IR (KBr): ν (cm⁻¹) 3272w, 3077w, 2933w, 1663s, 1626s, 1589s, 1568s, 1511s, 1474m, 1407m, 1366m, 1310m, 1268s, 1167m, 1072m, 987m, 708s.

Synthesis of complex Fe(**2**)₂

A solution of Fe(HMDS)₂ (34.4 mg, 0.091 mmol) in THF (12 mL) was added to a solution of **2** (60 mg, 0.183 mmol) in THF (8 mL). The resulting solution was stirred overnight at room temperature and then all the volatiles were removed under reduced pressure. The dark solid was dissolved in THF (10 mL), layered with hexane (10 mL) and kept at -20 °C for 24 hours to yield the pure product as dark blue crystals. Yield: 48.5 mg (75%). X-ray diffraction suitable crystals were grown from layering a THF solution of complex Fe(**2**)₂ with *n*-pentane at room temperature. The complex crystallizes with a solvent molecule as Fe(**2**)₂·0.5thf. The THF molecule is disordered over an inversion center and the positions are occupied by factor 0.5. Complex Fe(**2**)₂ can alternatively be synthesized using FeCl₂ as iron(II) precursor. Thus, a solution of LiHMDS (26.8 mg, 0.152 mmol) in THF (5 mL) was added to a solution of **2** (50 mg, 0.152 mmol) in THF (12 mL). The resulting blue solution, was poured over a suspension of FeCl₂ (9.6 mg, 0.076 mmol) in THF (5 mL) with triethylamine (42 μL, 0.304 mmol) and the mixture was stirred overnight. After removing all the volatiles under reduced pressure, dichloromethane was added in order to dissolve Fe(**2**)₂ and remove LiCl by filtration. Then, dichloromethane was removed under reduced pressure and the product purified as described above. Elemental analysis: calcd (%) for C₄₂H₃₀FeN₄O₄: C, 70.99; H, 4.26; N, 7.88; found: C,

70.60; H, 4.64; N, 7.42. ¹H NMR (500.13 MHz, THF-*d*₈): δ (ppm) 57.32 (*W*_{1/2} = 298 Hz, bs), 32.39 (*W*_{1/2} = 242 Hz, bs), 20.86 (*W*_{1/2} = 112 Hz, bs), 18.48 (*W*_{1/2} = 213 Hz, bs), 9.67 (*W*_{1/2} = 77 Hz, s), -17.64 (*W*_{1/2} = 157 Hz, bs), -21.20 (*W*_{1/2} = 337 Hz, bs), -43.58 (*W*_{1/2} = 1955 Hz, bs). 5 signals not located. ESI-MS: calcd (*m/z*) for C₄₂H₃₀FeN₄O₄⁺: 710.16110; found: 710.16465 [M]⁺. IR (THF solution): ν (cm⁻¹) 2924w, 2854w, 1643m, 1579m, 1518m, 1486m, 1444m, 1411m, 1347m, 1307m, 1256m, 1230m, 1160w, 1092w, 1070w, 1001w, 917w, 775w, 711w.

General procedures for the catalytic hydrosilylation of carbonyl compounds

Inside the glovebox, compound Fe(**2**)₂ (0.25-0.50 mol %) was dissolved in THF (2 mL) inside a small vial. The corresponding silane (0.63 mmol) was then added to the solution, followed by the carbonyl substrate (0.56 mmol), and the vial was sealed. The resulting mixture was stirred at room temperature during the times indicated in Tables 2 or 3 and then the reaction was quenched by adding HCl(aq) 1M (2 mL) and stirred for 30 min. to ensure the complete hydrolysis of the silyl ether product. The mixture was then taken to pH 7 by adding NaOH(aq) 5M and the organic products extracted with ethyl acetate (3x15 mL). The organic layers were dried using anhydrous Na₂SO₄, filtered and concentrated by rotatory evaporation. Quantitative NMR was applied for conversion determination. Isolated products were obtained after column chromatography in silica gel using ethyl acetate/hexane or dichloromethane as eluent.

General procedure for NMR monitored hydrosilylation reactions

Compound Fe(**2**)₂ (0.05-0.50 mol%) was put inside a J. Young screw-capped NMR sample tube and dissolved in THF-*d*₈ (1 mL). The corresponding silane (0.63 mmol) was then added to the solution, followed by the carbonyl substrate (0.56 mmol), and the tube was closed. The sample tube was shaken to ensure the homogeneity of the mixture and then placed inside the NMR spectrometer, where remained for the entire duration of the reaction monitoring.

Quantitative NMR acquisition parameters

¹H NMR determination of product's conversion was carried out by comparing signals arising from both carbonyl substrate and product. The standard acquisition parameters were one-dimensional pulse sequence which includes a 30° flip angle (Bruker zg30), recycle time (D1 = 30 s), time domain (TD = 64k), number of scans (NS = 1), acquisition time (AQ = 2.97 s), transmitter (frequency) offset (O1P = 8.0 ppm), and spectral width (SW = 22.0 ppm).

Single Crystal X-ray Diffraction

Ligand 2. X-ray data collection of suitable single crystal was done at 100(2) K on a Bruker VENTURE area detector equipped with graphite monochromated Mo-Kα radiation (λ = 0.71073 Å) by applying the ω-scan method. The data reduction was performed with the APEX2²⁷ software and corrected for absorption using SADABS.²⁸ Crystal structure was solved by direct methods using the SIR97 program²⁹ and refined by full-

matrix least-squares on F2 including all reflections using anisotropic displacement parameters by means of the WINGX crystallographic package.³⁰ All hydrogen atoms were included as fixed contributions riding on attached atoms with isotropic thermal displacement parameters 1.2 times or 1.5 times those of their parent atoms for the organic ligand except for hydrogen atom pertaining to N1.

Fe(2)2•0.5thf. Data was collected at 100(2) K on an STOE IPDS II diffractometer using Mo-K α radiation (λ = 71.073 pm) and ω -scan rotation. The structure was solved by direct methods and the refinement of all non-hydrogen atoms was performed with SHELX-97.³¹ All non-hydrogen atoms were refined with anisotropic thermal parameters. Hydrogen atoms were calculated on idealized positions using a riding model. The structure figures were generated with ORTEP.³² Details of the structure determination and refinement of **2** and Fe(**2**)₂•0.5thf are summarized in Table S1–S4. The supplementary crystallographic data have been deposited with the Cambridge Crystallographic Data Centre (CCDC numbers 1576113 and 1577523, respectively).

Conclusions

The synthesis and characterization of a highly active Fe(II) catalyst for the hydrosilylation of aldehydes and ketones have been described. Ligand deprotonation by two alternative methods resulted in a redox innocent amino-anthraquinonic chelate with TOFs of up to 63 min⁻¹ using very mild conditions such as 0.25 mol% of catalyst, room temperature, and even under solvent-free conditions. The catalyst has also been found to tolerate a range of functional groups where aldehydes are the most rapidly reduced and nitrogen-based derivatives the slowest. Kinetic studies have proven the rate-determining step to be subject to silane concentration first order dependence, and zeroth or first order in ketone when (EtO)₂MeSiH or Ph₂SiH₂ are employed, respectively. Investigations into the enantioselectivity of these reactions are currently undergoing in our laboratory.

Conflicts of interest

There are no conflicts to declare.

Acknowledgements

This work was supported by the Junta de Andalucía (Spain) under the project number P12-FQM-2668. A. R-B., R. L-R, and P. O-B thank the University of Almería and MEC for Ph.D. fellowships and a Ramón y Cajal contract (RYC-2014-16620), respectively.

Notes and references

- a) V. B. Pukhnarevich, E. Lukevics, L. I. Kopylova, M. G. Voronkov, *Perspectives of Hydrosilylation*, Institute of Organic Synthesis, Riga, Latvia, 1992; b) I. Ojima, Z. Li, J. Zhu, In *The Chemistry of Organic Silicon Compounds*; Z. Rappoport, Y. Apeloig, Eds.; John Wiley & Sons: New York, 1998; Vol. 2; c) H. Nishiyama, K. Itoh, In *Catalytic Asymmetric Synthesis*; I. Ojima, Ed.; Wiley-VCH: New York, 2000.
- a) H. Koinuma, F. Kawakami, H. Kato and H. Hirai, *J. Chem. Soc., Chem. Commun.*, 1981, 213; b) T. Matsuo and H. Kawaguchi, *J. Am. Chem. Soc.*, 2006, **128**, 12362; c) A. K. Roy, *Adv. Organomet. Chem.* 2008, **55**, 1; d) S. N. Riduan, Y. G. Zhang and J. Y. Ying, *Angew. Chem., Int. Ed.*, 2009, **48**, 3322; e) A. Berkefeld, W. E. Piers and M. Parvez, *J. Am. Chem. Soc.*, 2010, **132**, 10660; f) M. Khandelwal and R. J. Wehmschulte, *Angew. Chem., Int. Ed.*, 2012, **51**, 7323; g) R. Lalrempuia, M. Iglesias, V. Polo, P. J. S. Miguel, F. J. Fernández-Álvarez, J. J. Pérez-Torrente and L. A. Oro, *Angew. Chem., Int. Ed.*, 2012, **51**, 12824; h) S. Park, D. Bézier and M. Brookhart, *J. Am. Chem. Soc.*, 2012, **134**, 11404; i) W. Sattler and G. Parkin, *J. Am. Chem. Soc.*, 2012, **134**, 17462; j) K. Motokura, D. Kashiwame, A. Miyaji and T. Baba, *Org. Lett.*, 2012, **14**, 2642; k) A. Berkefeld, W. E. Piers, M. Parvez, L. Castro, L. Maron and O. Eisenstein, *Chem. Sci.*, 2013, **4**, 2152; l) O. Jacquet, C. D. Gomes, M. Ephritikhine and T. Cantat, *ChemCatChem*, 2013, **5**, 117; m) F. J. Fernández-Álvarez, A. M. Aitani, L. A. Oro, *Catal. Sci. Technol.* 2014, **4**, 611; n) Q. Liu, L. Wu, R. Jackstell, M. Beller, *Nat. Commun.* 2015, **6**, 5933; o) D. W. Stephan, *Acc. Chem. Res.* 2015, **48**, 306.
- M. C. Lipke, A. L. Liberman-Martin, T. D. Tilley, *Angew. Chem. Int. Ed.* 2017, **56**, 2260, and references cited therein.
- G. Du, M. M. Abu-Omar, *Organometallics* 2006, **25**, 4920.
- a) D. J. Parks, W. E. Piers, *J. Am. Chem. Soc.* 1996, **118**, 9440; b) D. J. Parks, J. M. Blackwell, W. E. Piers, *J. Org. Chem.* 2000, **65**, 3090.
- Selected references: a) Piers, W. E.; Marwitz, A. J. V.; Mercier, L. G. *Inorg. Chem.* 2011, **50**, 12252; b) Oestreich, M.; Hermeke, J.; Mohr, J. *Chem. Soc. Rev.* 2015, **44**, 2202; c) Peng, M. Zhang, Z. Huang, *Chem. Eur. J.* 2015, **21**, 14737; d) L. Süsse, J. Hermeke, M. Oestreich, *J. Am. Chem. Soc.* 2016, **138**, 6940.
- a) B. Marciniak, J. Gulinsky, W. Urbaniak, Z. W. Kornetka, In *Comprehensive Handbook on Hydrosilylation*; B. Marciniak, Ed.; Pergamon: Oxford, 1992; b) B. Marciniak, *Hydrosilylation: A Comprehensive Review on Recent Advances*; Ed.; Springer: New York, 2009. For reviews of iron-catalyzed hydrosilylation: c) R. H. Morris, *Chem. Soc. Rev.* 2009, **38**, 2282; d) M. Zhang, A. Zhang, *Appl. Organomet. Chem.* 2010, **24**, 751; e) K. Junge, K. Schroder, M. Beller, *Chem. Commun.* 2011, **47**, 4849.
- a) S. K. Ritter, Iron's Star Rising. *Chem. Eng. News*, July 28, 2008, **86**, 53; b) R. M. Bullock, *Catalysis without precious metals*; Wiley-VCH: Weinheim, 2010.
- a) S. Enthaler, K. Junge, M. Beller, In *Iron Catalysis in Organic Chemistry*; B. Plietker, Ed.; Wiley-VCH: Weinheim, 2008; pp

- 125-145; b) S. Enthaler, K. Junge, M. Beller, *Angew. Chem. Int. Ed.* 2008, **47**, 3317; c) S.L. Buchwald, C. Bolm, *Angew. Chem., Int. Ed.* 2009, **48**, 5586; d) E. Nakamura, N. Yoshikai, *J. Org. Chem.* 2010, **75**, 6061; e) C.-L. Sun, B.-J. Li, Z.-J. Shi, *Chem. Rev.* 2011, **111**, 1293; f) K. Junge, K. Schröder, M. Beller, *Chem. Commun.* 2011, 4849; g) O.G. Mancheño, *Angew. Chem., Int. Ed.* 2011, **50**, 2216.
- 10 Selected references on Fe-catalyzed hydrosilylations: a) H. Nishiyama, A. Furuta, *Chem. Commun.* 2007, 760; b) N. S. Shaikh, K. Junge, M. Beller, *Org. Lett.* 2007, **9**, 5429; c) A. Furuta, H. Nishiyama, *Tetrahedron Lett.* 2008, **49**, 110; d) A.M. Tondreau, E. Lobkovsky, P.J. Chirik, *Org. Lett.* 2008, **10**, 2789; e) N. S. Shaikh, S. Enthaler, K. Junge, M. Beller, *Angew. Chem., Int. Ed.* 2008, **47**, 2497; f) B. K. Langlotz, H. Wadepohl, L. H. Gade, *Angew. Chem., Int. Ed.* 2008, **47**, 4670. g) T. Inagaki, A. Ito, J. Ito, H. Nishiyama, *Angew. Chem., Int. Ed.* 2010, **49**, 9384; h) V. V. K. M.Kandepi, J. M. S. Cardoso, E. Peris, B. Royo, *Organometallics* 2010, **29**, 2777; i) P. Bhattacharya, J. A. Krause, H. Guan, *Organometallics* 2011, **30**, 4720; f) F. Jiang, D. Bézier, J.-B. Sortais, C. Darcel, *Adv. Synth. Catal.* 2011, **353**, 239; g) D. Bézier, F. Jiang, T. Roisnel, J.-B. Sortais, C. Darcel, *Eur. J. Inorg. Chem.* 2012, 1333; h) T. Hashimoto, S. Urban, R. Hoshino, Y. Ohki, K. Tatsumi, F. Glorius, *Organometallics* 2012, **31**, 4474; i) E. Buitrago, F. Tinnis, H. Adolfsson, *Adv. Synth. Catal.* 2012, **354**, 217; j) B. Blom, S. Enthaler, S. Inoue, E. Irran, M. Driess, *J. Am. Chem. Soc.* 2013, **135**, 6703; k) Z. Zuo, H. Sun, L. Wang, X. Li, *Dalton Trans.* 2014, **43**, 11716; l) Z. Zuo, L. Zhang, X. Leng, Z. Huang, *Chem. Commun.* 2015, **51**, 5073; m) F. S. Wekesa, R. Arias-Ugarte, L. Kong, Z. Sumner, G. P. McGovern, M. Findlater, *Organometallics* 2015, **34**, 5051; n) T. C. Jung, G. Argouarch, P. Weghe, *Catal. Commun.* 2016, **78**, 52; o) B. Xue, H. Sun, O. Niu, X. Li, O. Fuhr, D. Fenske, *Catal. Commun.* 2017, **94**, 23.
- 11 S. Warratz, L. Postigo, B. Royo, *Organometallics*, 2013, **32**, 893.
- 12 J. Yang, T. D. Tilley, *Angew. Chem. Int. Ed.* 2010, **49**, 10186.
- 13 A. M. Tondreau, J. M. Darmon, B. M. Wile, S. K. Ford, E. Lobkovsky, P. Chirik, *Organometallics*, 2009, **28**, 3928.
- 14 M. Kadarkaisamy, D. Mukherjee, C. C. Soh, A. G. Sykes, *Polyhedron* 2007, **26**, 4085, and references cited therein.
- 15 A. Raya-Barón, M. A. Ortuño, P. Oña-Burgos, A. Rodríguez-Diéguez, R. Langer, C. J. Cramer, I. Kuzu, I. Fernández, *Organometallics* 2016, **35**, 4083.
- 16 D. Barasch, O. Ziporia, I. Ringel, I. Ginsburg, A. Samuni, J. Katzhendler, *Eur. J. Med. Chem.* 1999, **34**, 597.
- 17 T. Moriuchi, T. Watanabe, I. Ikeda, A. Ogawa, T. Hirao, *Eur. J. Inorg. Chem.* 2001, 277.
- 18 Y. García, G. Bravic, C. Gieck, D. Chasseau, W. Tremel, P. Gutlich, *Inorg. Chem.* 2005, **44**, 9723.
- 19 A. J. Ruddy, C. M. Kelly, S. M. Crawford, C. A. Wheaton, O. L. Sydora, B. L. Small, M. Stradiotto, L. Turculet, *Organometallics* 2013, **32**, 5581.
- 20 T. K. Mukhopadhyay, M. Flores, T. L. Groy, R. J. Trovitch, *J. Am. Chem. Soc.* 2014, **136**, 882.
- 21 A. A. Mikhailine, M. I. Maishan, A. J. Lough, R. H. Morris, *J. Am. Chem. Soc.* 2012, **134**, 12266.
- 22 M. A. Watzky, R. G. Finke, *J. Am. Chem. Soc.* 1997, **119**, 10382, and references cited therein.
- 23 T. Bleith, L. H. Gade, *J. Am. Chem. Soc.* 2016, **138**, 4972.
- 24 A. B. Pangborn, M. A. Giardello, R. H. Grubbs, R. K. Rosen, F. J. Timmers, *Organometallics* 1996, **15**, 1518.
- 25 R. A. Andersen, J. R. Knut Faegri, J. C. Green, A. Haaland, M. F. Lappert, W.-P. Leung, K. Rypdal, *Inorg. Chem.* 1988, **27**, 1782.
- 26 D. D. Perrin, W. L. F. Armarego, *Purification of Laboratory Chemicals*, 3rd ed.; Pergamon Press: Oxford, U.K., 1988
- 27 Bruker Apex2, Bruker AXS Inc., Madison, Wisconsin, USA, 2004.
- 28 G. M. Sheldrick, SADABS, Program for Empirical Adsorption Correction, Institute for Inorganic Chemistry, University of Göttingen: Germany, 2016.
- 29 A. Altomare, M. C. Burla, M. Camilla, G. L. Cascarano, C. Giacovazzo, A. Guagliardi, A. G. G. Moliterni, G. Polidori, R. Spagna, SIR97: a new tool for crystal structure determination and refinement. *J. Appl. Crystallogr.* 1999, **32**, 115.
- 30 a) G. M. Sheldrick, SHELX-2014, Program for Crystal Structure Refinement; University of Göttingen, Göttingen, Germany, 2014. b) Farrugia, L. J. WinGX suite for small-molecule single-crystal crystallography. *J. Appl. Cryst.* 1999, **32**, 837.
- 31 SHELX includes SHELXS97, SHELXL97: G. M. Sheldrick, *Acta Crystallogr., Sect. A* 2008, **64**, 112.
- 32 ORTEP3 for Windows: L. J. Farrugia, *J. Appl. Crystallogr.* 1997, **30**, 565.

For the Table of Contents:

Put some iron-anthraquinoid in your chemistry. The synthesis and characterization of a highly active Fe(II) catalyst for the hydrosilylation of aldehydes and ketones have been described.

